J. S. Afr. Inst. Min. Metall., vol. 85, no. 2.
Feb. 1985. pp. 51-63.

The lifting action of lifter bars in rotary mills

by L.A. VERMEULEN*

SYNOPSIS

A simple argument shows that it is impossible for the flight of a rod in contact with a lifter bar in a rotary mill to be initiated at that point on the upside of mill rotation when all the forces acting on the rod are in equilibrium. The argument was confirmed experimentally in a study showing that the lift of lifter bars is a function of their height, that the rod velocity at the point of departure has a significant radial component, and that the subsequent flight of a rod is along a parabolic trajectory as predicted by elementary mechanics.

A quantitative account of the observed effects, which is based on a dynamic theory of the sliding interaction between rods and lifter bars, revealed interesting properties of the motions of rods down the surfaces of lifter bars when the latter are in uniform circular motion during the rotation of a mill.

SAMEVATTING

'n Eenvoudige redenasie toon dat dit onmoontlik vir die vlug van 'n stang in aanraking met 'n ligstaaf in 'n draaimeul is om by 'n punt aan die bokant van die meulrotasie te begin wanneer al die kragte wat op die stang inwerk, in ewewig is. Die redenasie is eksperimenteel bevestig in 'n studie wat toon dat die lighoogte van ligstawe 'n funksie van hul hoogte is; dat die stangsnelheid by die vertrekpunt 'n beduidende radiale komponent het; en dat die daaropvolgende vlug van 'n stang langs 'n paraboliese baan is soos deur elementêre meganika voorspel.

'n Kwantitatiewe verslag oor die waargenome gevolge, wat gebaseer is op 'n dinamiese teorie van die skuifwisselwerking tussen stange en ligstawe, het interessante eienskappe aan die lig gebring van die beweging van die stange teen die oppervlak van die ligstawe wanneer laasgenoemde, tydens die rotasie van 'n meul in 'n eenvormige sirkelbeweging is.

Introduction

The lifter bars in a rotary mill are steel castings of rectangular cross-section. The practice is to clamp these objects to the liner blocks and mill shell in such a manner that a line of symmetry through the protrusion of the lifter bar is radial. The situation is shown in Fig. 1, in which some of the details have been omitted and the size of the grinding element and lifter bar relative to that of the mill have been exaggerated in order to reveal certain features important to the present discussion. Fig. 1 shows that the normal reaction, N, is not perpendicular to the radius vector passing through the centre of a grinding element in contact with a lifter bar, but that it has a radial component,

$$N \sin \beta = \frac{N(a + \frac{1}{2}d)}{R-a},$$

where R is the internal mill radius, a is that of the grinding element, d is the width of the lifter bar, and β is the angle between the given radius vector and the surface of the lifter bar. It is shown later that this radial component of the normal reaction accounts for more than 20 per cent of the lift of standard lifter bars in a rod mill

For the sake of being definite, the present discussion refers to the action of lifter bars on rods, but many of the conclusions are also applicable to other types of grinding media, e.g. balls or pebbles.

To define the lifting action of lifter bars in a quantitative way, a hypothetical situation is first considered in which an isolated rod is 'keyed' in to the rotary motion of a mill.

While the rod is in contact with the liner and at an angle ϕ to the horizontal, the net radial force, F_r, on the rod is

$$F_r = m\Omega^2(R-a) - mg \sin \phi, \quad \ldots\ldots\ldots\ldots \quad (1)$$

where Ω is the angular velocity of mill rotation, g is the gravitational acceleration, and m is the mass of the rod.

At the so-called angle of departure, ϕ_d, the radial force is zero, and the flight of the rod back into the body of the mill can be initiated with the following equations of motion:

$$X(t) = X_d + V_{dx}t, \quad \ldots\ldots\ldots\ldots\ldots \quad (2)$$

$$Y(t) = Y_d + V_{dy}t - \tfrac{1}{2}gt^2, \quad \ldots\ldots\ldots\ldots \quad (3)$$

where X_d and Y_d are the coordinates of the rod centre when

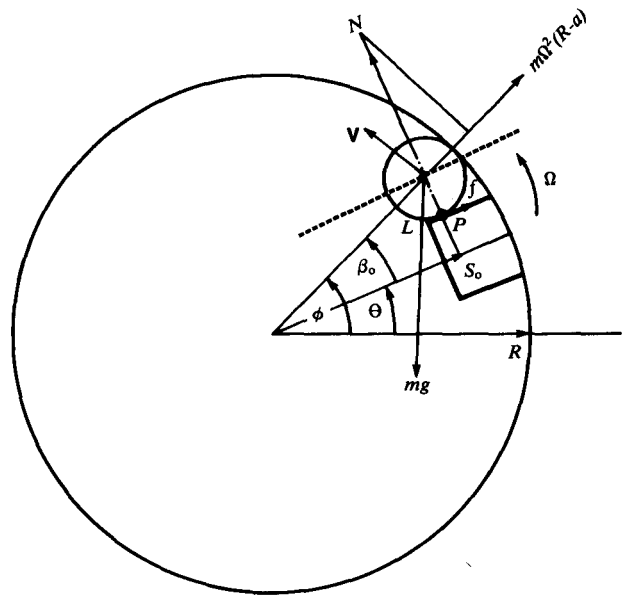

Fig. 1—Interaction of a rod and a lifter bar. The sizes of the rod and the lifter bar relative to the mill have been exaggerated to reveal that, when the lifter bar is at angle θ, the rod is at angle φ and the normal reaction *N* has a component along the radius vector through the rod centre. *P* is the point of contact between the rod and the surface of the lifter bar, and *L* is the edge of the lifter bar.

* Chief Scientist, Council for Mineral Technology (Mintek), Private Bag X3015, Randburg, 2125 South Africa.

SA ISSN 0038-223 X /$3.00 + 0.00.

it is at the angular position ϕ_d at $t = 0$. The initial velocity is

$$\mathbf{V}_d = \Omega(R-a)\,\hat{\phi}_d, \quad \ldots\ldots\ldots\ldots\ldots\ldots \quad (4)$$

where $\hat{\phi}_d$ is a unit vector in the direction of mill rotation and normal to the radius vector inclined at an angle ϕ_d to the horizontal. If V_{dx} and V_{dy} are the horizontal and vertical components of $\mathbf{V}_d$,

$$V_{dx} = \Omega(R-a)\sin\phi_d = -\Omega Y_d, \quad \ldots\ldots\ldots \quad (5)$$

$$V_{dy} = \Omega(R-a)\cos\phi_d = \Omega X_d. \quad \ldots\ldots\ldots \quad (6)$$

Equations (2) and (3) are parametric equations for the flight of the rod along a parabolic trajectory whose equation with respect to horizontal and vertical axes at the mill centre is

$$Y(X) = Y_d - \cot\phi_d(X-X_d) - \tfrac{1}{2}g(X-X_d)^2/V_{dx}^2. \quad (7)$$

The effect of lifter bars is to increase the angle of departure of the rod to a value ϕ_F. Indeed, the lift (L) of lifter bars can be defined as

$$L = \phi_F - \phi_d. \quad \ldots\ldots\ldots\ldots\ldots\ldots \quad (8)$$

In rod mills, the height of standard new lifter bars is about 70 per cent of the diameter of a new rod, and their widths are about equal to the diameter of a new rod. They provide a lift of about 20°.

A recent publication[1] has not only taken into account the fact that the surfaces of lifter bars are not radial, but has also allowed for friction in a consideration of the particle take-off conditions in a lined mill. From Fig. 1, it can be seen that the vector sum of all the forces acting on the rod is zero when

$$m\Omega^2(R-a)\cos\beta_0 + \mu N - mg\sin\theta_0 = 0 \quad \ldots\ldots \quad (9)$$

$$N - mg\cos\theta_0 + m\Omega^2(R-a)\sin\beta_0 = 0, \quad \ldots\ldots \quad (10)$$

where N is the normal reaction, μ is the coefficient of friction, and θ_0 is the angular position of the lifter bar when these conditions are satisfied. Fig. 1 shows that, when the lifter bar is at θ_0, the rod is at the angular position

$$\phi_0 = \theta_0 + \beta_0. \quad \ldots\ldots\ldots\ldots\ldots\ldots \quad (11)$$

At that point, the velocity is

$$\mathbf{V}_{rod} = \Omega(R-a)\,\hat{\phi}_0. \quad \ldots\ldots\ldots\ldots\ldots \quad (12)$$

It is generally thought that the rod is projected into flight from this position, at which the vector sum of all the forces on the rod is zero and its velocity is finite and purely tangential. With the milling parameters used here, for which

$\frac{1}{2}d \approx a$, and

$R \approx 27a$,

which are realistic proportions, it is found from equations (9), (10), and (11) that, when μ is zero,

$$\phi_0 - \phi_d \approx 4{,}3°.$$

This contribution of more than 20 per cent of the lift is entirely due to the radial component of the normal reaction. Also, from equations (9), (10), and (11), if $\mu = 0{,}3$,

$$\phi_0 - \phi_d \approx 20°.$$

Thus, if flight is initiated at ϕ_0, the observed lift of standard lifter bars can apparently be accounted for by a coefficient of friction with a value of 0,3.

The above calculations, which are very similar to those given by McIvor[1], who also quoted a value of 0,3 for the coefficient of friction, do not provide an explanation for the lift of lifter bars. It is impossible for a rod to depart from the lifter bar when the angle ϕ_0 is achieved for, if it did, then after a very short time Δt, the lifter bar would catch up with the rod. Qualitatively, this is generally because some of the kinetic energy of the rod during its flight is continuously converted into potential energy. More explicitly, after time interval Δt, the speed of the rod would be

$$V_{rod} < \Omega(R-a)\left(1 - \frac{g\Delta t\cos\phi_0}{\Omega(R-a)}\right), \quad \ldots\ldots\ldots \quad (13)$$

but the velocity of the point P on the lifter bar, the point with which the rod *was* in contact, would be

$$\mathbf{V}_p = \hat{\alpha}\,\Omega(R-a), \quad \ldots\ldots\ldots\ldots\ldots\ldots \quad (14)$$

where the angle α is $\phi_0 - \frac{1}{2}\beta_0$ when $\frac{1}{2}d$ is equal to a.

Since the magnitude of $\mathbf{V}_{rod}$ is smaller than that of $\mathbf{V}_p$ and its direction is nearly parallel to that of the latter (because in practice angle β_0 is small), it is clear that the lifter bar will tend to overtake the rod. Therefore, after conditions (9) and (10) have been satisfied, the rod will not be projected into flight, but will either slip or roll down the surface of the lifter bar until it reaches the edge of the lifter bar at L.

Moreover, in contrast to the generally held supposition that the rod velocity is purely tangential at the point where flight is initiated, it is shown later that the velocity is not purely tangential but it has a significant radial component associated with it.

The aim of the present work was to explore the nature of the interaction of rods and lifter bars. An experimental mill was used, and the motions of rods were recorded with a ciné camera. The interactions were emphasized by the use of lifter bars of various heights; in some cases they were proportionately much higher than those used in industrial mills.

Apparatus and Methods

The study was made of the motions of rods in an experimental rotary mill that was fitted with transparent windows. The camera speed was nominally 64 frames per second, and the mill speed was nominally 60 r/min. The mill was 260 mm long with an internal diameter of 263 mm. It was charged to a height of 45 per cent of its diameter with 9,5 mm rods 250 mm in length. The charge, the operating speed (nominally about 72 per cent of the critical speed), and the ratio of mill diameter to rod diameter were therefore comparable with those of an industrial rod mill.

The mill was operated with a smooth inner lining and with sixteen rows of lifter bars so that the effect of the latter on the motion of the charge could be studied.

Images from the film strips were projected onto large sheets of graph paper by means of a slide projector. In that way it was possible to record the positions of rods in successive frames of the film strip. Some minor difficulties were experienced with thermal distortion of the film as a result of

heating by the projector lamp. A further distortion was introduced by the need in the experiments for the camera to be held slightly to one side of the mill axis so that a clear view would be obtained of the tumbling charge, with the consequence that the mill images were slightly oval rather than circular. In the images, the ratio of maximum to minimum diameters was 1,014. As a result, unavoidable experimental errors were associated with the determinations of the positions and speeds of the rods. Assessments of the measurements taken have suggested that the uncertainties in r and ϕ, the polar coordinates of a rod, were 2 mm and 3° respectively, and that the uncertainty in the determinations of the speed of a rod was about 10 per cent. A considerable proportion of the latter error is due to uncertainties associated with the position of the rod, the rotational speed of the mill, and the number of frames per second of the ciné film. With the aid of a marker on the mill, it could be established that 72 frames corresponded to one rotation of the mill.

It is also to be noted that the lifter bars were rectangular in cross-section, their widths were approximately equal to the diameter of a rod, and they were clamped to the shell in the symmetrical manner previously described, i.e. so that lines of symmetry through the lifting protrusions were radial. The situation, which corresponds to an industrial mill fitted with new lifter bars, is shown in Fig. 1.

Results

Measurements were made of the angular positions of the rods when they departed from the lifter bars. When groups of rods were involved, the angles of departure were larger than in situations when a single rod was in contact with a lifter bar. It was anticipated that the mechanics associated with groups of rods would be fairly complex, and attempts were therefore made to obtain representative measurements of situations in which only one rod was involved so that the observed effects could be analysed.

Table I shows the angles of departure of isolated rods from the lifter bars in the experimental mill, and also the angle of departure of the rods from the mill. It shows that the angle of departure is not only strongly affected by the lifter bars but that the angle, and therefore the lift, depends upon their height. This observation is entirely in accord with the expectation that the rod will either slip or roll down the surface of the lifter bar. With the lowest lifter bars, the lift was 20°.

The path of an isolated rod in the mill when the latter was fitted with the highest lifter bars is shown in Fig. 2. The motion of this rod was followed for sixteen successive

TABLE I
MEASURED LIFT OF LIFTER BARS IN THE EXPERIMENTAL ROD MILL

Height of lifter bar, h	Observed	
	Angle of departure $\phi_F(h)$	Lift, L
mm	degree	degree
Zero	32 ± 4	—
6,3	52 ± 3	20
12,7	67 ± 3	35
20,0	73 ± 3	41

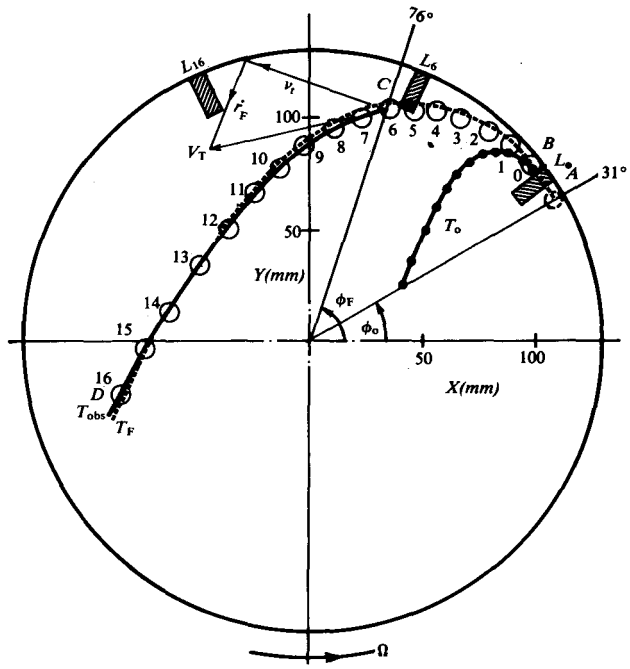

Fig. 2—The path of a rod in an experimental mill when the latter is fitted with high lifter bars. The circles are measured rod positions at consecutive times, and the dotted curve is the path predicted by the dynamics of a sliding interaction between rod and lifter bar between positions A and C. At angular position ϕ_o, the forces on the rod are in equilibrium and, at ϕ_F, when the rod is just free of the lifter bar, the radial component of the velocity is more than 50 per cent of its tangential component.

frames from the time it occupied position B. Also shown are some positions, L, of the lifter bar that was in contact with the rod at various times. The scatter associated with the measurements, due to the circumstances previously described, is clearly visible. When the rod was at position 6, it was apparently still in contact with the lifter bar, but at position 7 it was definitely free of the lifter bar. Considerations of the trajectory between these two positions show that, at the point of departure, the velocity of the rod has a substantial radial component, which is about 50 per cent of the tangential component. Although the radial component of the rod velocity is emphasized when the lifter bars are high as in Fig. 1, it is still significant when the height of the lifter bars is typical.

Discussion

As shown in Fig. 2, the rod is undoubtedly in flight between positions 7 and 16. It is of interest to analyse the trajectory in this range, to confirm that it is indeed parabolic as predicted by equations (2), (3), and (7), and to determine the magnitude and direction of the initial velocity at the point where flight was initiated.

Equations (3) and (7) were fitted to numerical data describing the positions of the rod by use of a non-linear least-squares-fit computer program. The computations yielded the following:

$$Y(t') = (100{,}8 \pm 0{,}3) - (4{,}56 \pm 0{,}06)t' - (1{,}060 \pm 0{,}008)t'^2 \quad \ldots\ldots\ldots\ldots \quad (15)$$

$$Y(X) = (101{,}3 \pm 0{,}7) - (0{,}41 \pm 0{,}03)(X - X_7) - (7{,}2 \pm 0{,}3)(X - X_7)^2. \quad \ldots\ldots\ldots \quad (16)$$

The parabola described by equation (16) is shown in Fig. 2 by the continuous curve labelled T_{obs} (the observed trajectory). This curve is clearly an accurate description of the flight of the rod between positions 7 and 16.

It can therefore be concluded that the flight paths of isolated grinding elements in a rotary mill are indeed parabolic, as predicted by elementary theory. Some of the controversy that has existed in the past regarding the flight of balls in a rotary mill has been described by Taggart[2] and McIvor[1].

A comparison of equations (3) and (15), and of (7) and (16), shows that

$$\tfrac{1}{2}g = 1{,}060 \pm 0{,}008 \cdot \text{mm}\,\tau^{-2}, \quad \ldots\ldots\ldots\ldots \quad (17)$$

$$V_{7x} = -\sqrt{\frac{1{,}06}{7{,}21 \times 10^{-3}}}$$

$$= -12{,}1\ \text{mm} \cdot \tau^{-1} \text{ to about 5 per cent}, \quad \ldots\ldots \quad (18)$$

$$V_{7y} = -4{,}57\ \text{mm} \cdot \tau^{-1} \text{ to about } 1\tfrac{1}{2} \text{ per cent}, \quad \ldots\ldots \quad (19)$$

where τ is the time interval between frames of the ciné film.

It is satisfying that the standard deviation of g is less than 1 per cent. Since $\frac{1}{2}g$ is 4900 mm · s^{-2}, it follows that τ is about 1/68 s, and it is concluded that the film speed was 68 frames per second rather than the nominal speed of 64 frames per second. The discrepancy is about 6 per cent, and the implication is that the errors in V_{7x} and V_{7y} are somewhat larger than the standard deviations given in equations (15) and (16).

From the value of 68 frames per second, it is found that V_{7x} is -823 mm · s^{-1} and V_{7y} is 311 mm · s^{-1}. So, at position 7, the velocity of the rod was about 880 mm · s^{-1} at an angle of 21° below the negative X-direction, and it is estimated that the errors are about 10 per cent.

Since V_{7x} is negative, equation (2) shows that, for $t' > 7\tau$, the values of the X coordinate of the rod decrease linearly with time. This behaviour is confirmed in Fig. 3, which shows that the points corresponding to $t' > 7\tau$ are indeed linearly distributed, as predicted by equation (2). The slope of the linear portion of this graph yields

$$V_{7x} = -11{,}9\ \text{mm} \cdot \tau^{-1} = -809\ \text{mm} \cdot \text{s}^{-1}. \quad \ldots\ldots \quad (20)$$

The discrepancy between this and the previously obtained value for this quantity is less than 2 per cent.

Fig. 3 also shows that the data points for $t' < 6\tau$ depart from the straight line in a systematic manner. This is clear evidence that, between $B(t = 0)$ and the rod position defined by the angle ϕ_F, there is an interaction between the rod and the bar. There can be an interaction only if the rod is, in fact, in contact with the lifter bar during this angular range.

It is clear that, in this angular range, the contact point between the rod and the lifter bar is migrating down the surface of the bar, as suggested earlier. Therefore, even though the rod had already passed through the equilibrium position defined by ϕ_0, when the vector sum of all forces acting on it was zero, it continued to experience the normal reaction N until it left the lifter bar at the angular position ϕ_F.

During the given angular range, ϕ_0 to ϕ_F, the further

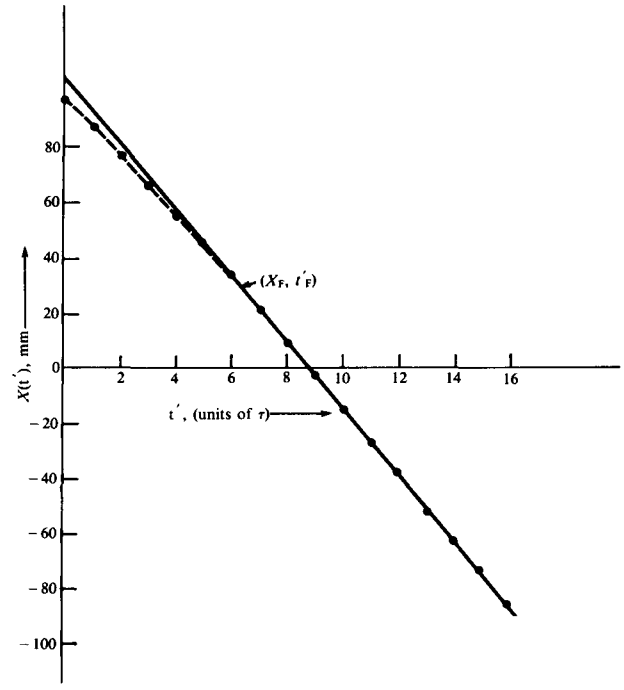

Fig. 3—The measured dependence of the X coordinate of the rod position on time t'. The dependence is linear for $t' > 7t$. The departure from linearity at shorter times indicates that there was an interaction between the rod and the lifter bar in the angular range B to C, shown in Fig. 2.

interaction could have been one in which the rod was either slipping or rolling down the surface of the lifter bar, or both. Although such interactions have not previously been considered in this connection, it is believed that it is one of these mechanisms that gives rise to the observed lift of lifter bars. The dynamics of the sliding interaction will be considered in some detail.

It has already been shown with reference to Fig. 1 that the vector sum of all the forces on the rod is zero when equations (9) and (10) are satisfied. From these conditions, one obtains

$$\Omega^2(R-a)(\cos\beta_0 - \mu\sin\beta_0) - g(\sin\theta_0 - \mu\cos\theta_0) = 0. \quad \ldots\ldots\ldots\ldots \quad (21)$$

This equation has to be solved numerically for θ_0 for given values of μ. For example, with the parameters of the experiment described here, it was found that, when $\mu = 0$, $\theta_0 \approx 27{,}01°$ but, when $\mu = 0{,}1$, then $\theta_0 \approx 32{,}36°$.

If $t = 0$ when $\theta = \theta_0$, and $t = t_L$ when the rod will have slid the full length of lifter-bar surface available to it, then Fig. 4 shows that the problem is simply one of sliding down an inclined plane whose inclination is increasing at a constant rate, namely Ω. In Fig. 4, the size of a rod and lifter bar relative to that of the mill were exaggerated so that the relationships between the various quantities could be established. For example, the diagram shows that, when the lifter bar is at angle $\theta(t)$ to the horizontal axis, the rod is at angle $\phi(t)$, with

$$\phi(t) = \theta(t) + \beta,$$

where β is time dependent, $\beta = \beta(t)$.

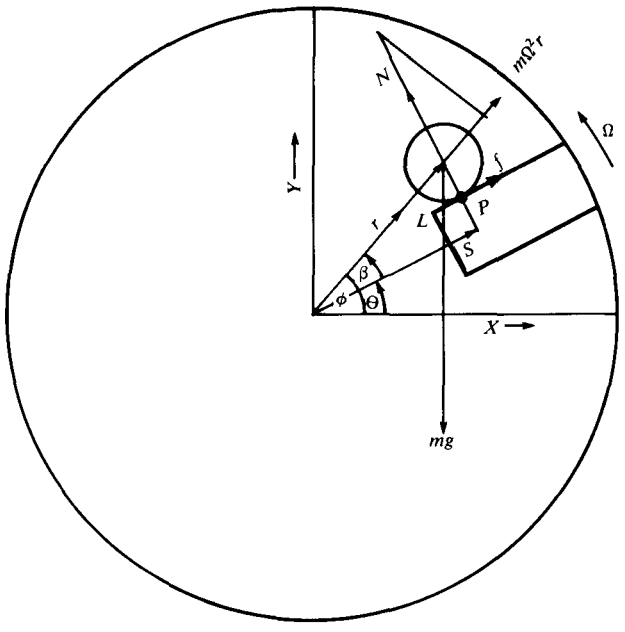

Fig. 4—A dynamic model of the sliding interaction. The diagram exaggerates the sizes of the rod and the lifter bar relative to that of the mill, and shows that angle β is a function of the rod position on the lifter bar.

However, at all times $0 < t < t_L$,

$$\mathbf{s} = \mathbf{r} \cos \beta, \quad \ldots \ldots \ldots \ldots \ldots \quad (23)$$

where **r** is the distance of the rod from the mill centre, **s** is a radius vector along the axis of the lifter bar as shown, and displacements $\triangle \mathbf{s}$ are along the surface of the lifter bar and are positive in the direction of increasing **s**.

Analysis of Fig. 4 shows that

$$m\Omega^2 r \cos \beta + \mu N - mg \sin (\Omega t + \theta_0) = m\frac{d^2 s}{dt^2} \quad \ldots (24)$$

$$N - mg \cos (\Omega t + \theta_0) + m\Omega^2 r \sin \beta = 0. \quad \ldots \ldots \quad (25)$$

The motion is therefore governed by the differential equation

$$\frac{d^2 s}{dt^2} - \Omega^2 s = g\{\mu \cos (\Omega t + \theta_0) - \sin (\Omega t + \theta_0)\} - \Omega^2 \delta, \quad \ldots \ldots \ldots \quad (26)$$

where $\delta = \mu r \sin \beta = \mu(a + \frac{1}{2}d)$.

The boundary conditions are that, at $t = 0$,

$$s(0) = (R-a) \cos \beta_0 \quad \ldots \ldots \ldots \ldots \quad (27)$$

$$\left(\frac{ds}{dt}\right)_{t=0} = 0. \quad \ldots \ldots \ldots \ldots \quad (28)$$

The solution to (26), which is consistent with the boundary conditions, is

$$s(t) = [s(0) - \delta + \frac{g}{2\Omega^2}(\mu \cos \theta_0 - \sin \theta_0)] \cosh \Omega t, - \frac{g}{2\Omega^2}[(\mu \sin \theta_0 + \cos \theta_0) \sinh \Omega t + \{\mu \cos(\Omega t + \theta) - \sin (\Omega t + \theta_0)\}] + \delta. \quad (29)$$

An expression for the rod speed relative to the surface of the lifter bar is useful. It is

$$\frac{ds}{dt} = \Omega[s(0) - \delta + \frac{g}{2\Omega^2}(\mu \cos \theta_0 - \sin \theta_0)] \sinh \Omega t - \frac{g}{2\Omega}(\mu \sin \theta_0 + \cos \theta_0) \cosh (\Omega t + \theta_0) - \{\mu \sin (\Omega t + \theta_0) + \cos (\Omega t + \theta_0)\}]. \quad (30)$$

Fig. 5 shows how the magnitudes of the displacements $s(t)$ from the mill centre, and the corresponding magnitudes of the displacements $\sigma(t)$ and $\varrho(t)$ from the inner lining, develop as a function of the time. The latter are defined by

$\sigma(t) = s_0 - s(t)$, and

$\varrho(t) = (R-a) - r(t)$.

When $s(t)$ is known, it becomes possible to display the acceleration of the rod down the surface of the lifter bar. It is shown in Fig. 6 that, at zero time, corresponding to the equilibrium position, the acceleration is zero because then the vector sum of all the forces on the rod is zero. Thereafter, the acceleration down the surface of the lifter bar increases with time because the component of the weight along the surface of the lifter bar increases steadily as the angular position of the bar increases and the displacement $s(t)$ becomes smaller.

The velocity of a rod while it is interacting with a lifter bar is also of interest. Before the rod passes through angle ϕ_0, its velocity is

$$\mathbf{V}_{rod} \ (\phi \leqslant \phi_0) = \Omega(R-a)\dot{\phi},$$

i.e. the velocity is purely tangential and of constant

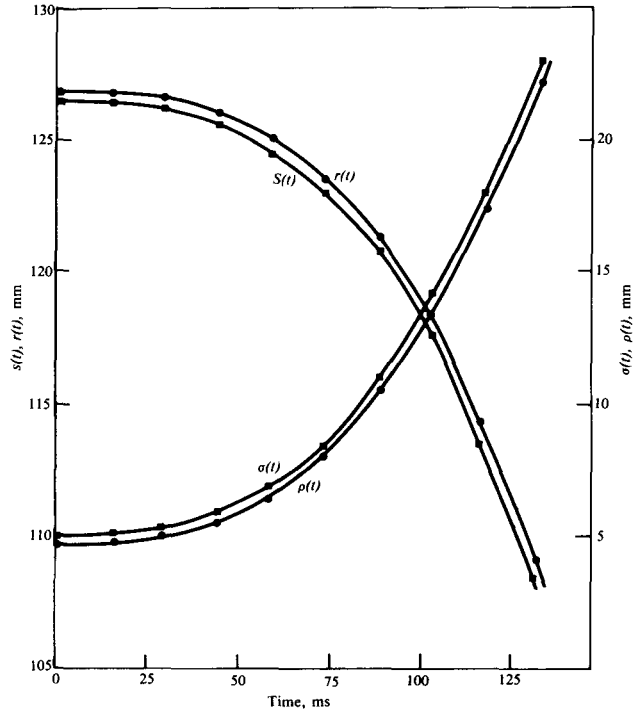

Fig. 5—Time dependence of the displacement of a rod while it is in contact with a lifter bar; $s(t)$ and $r(t)$ are measured from the axis, and $\sigma(t)$ and $\varrho(t)$ from the inner lining.

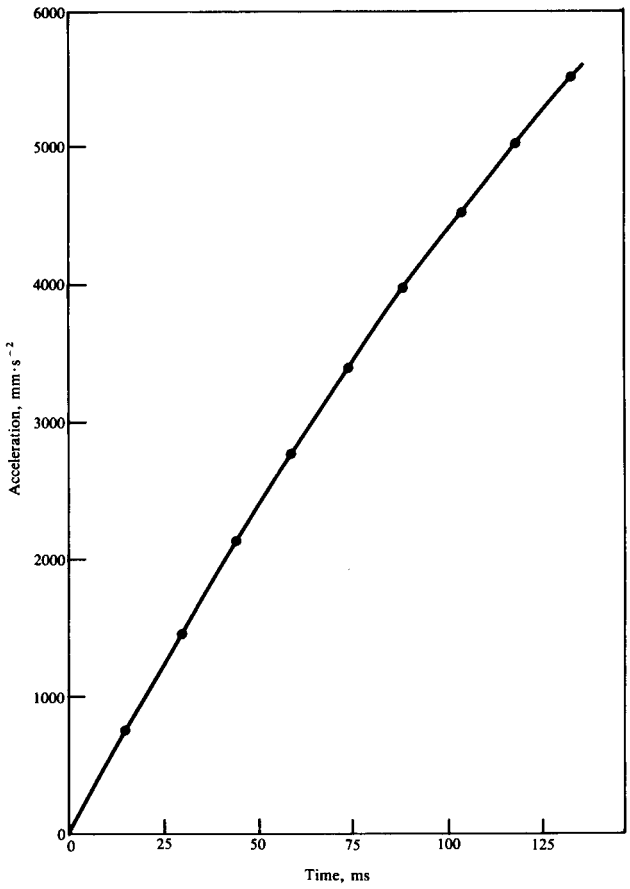

Fig. 6—Time dependence of the magnitude of acceleration of a rod down the surface of a lifter bar.

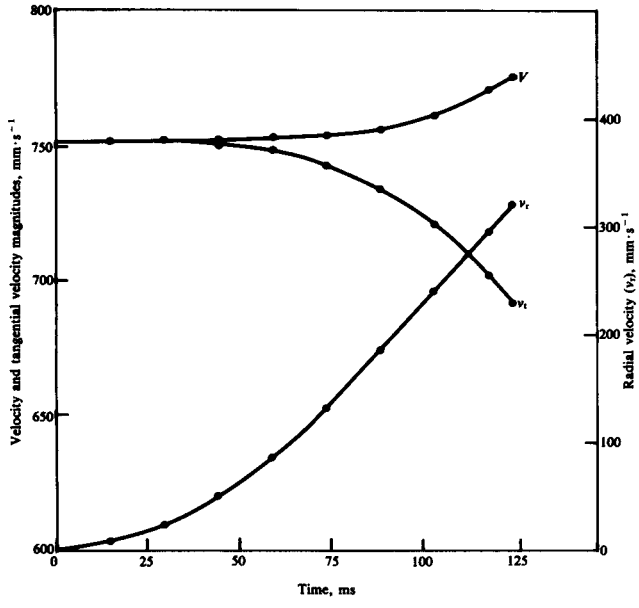

Fig. 7—Calculated time dependence of the magnitudes of the rod velocity (V) and of its radial (v_r) and tangential (v_t) components during the interaction between the rod and lifter bar. At about 29 ms after equilibrium, v_t passes through a maximum.

magnitude. However, after the rod has passed through the equilibrium angle ϕ_0, when it starts to slide down the lifter bar, the velocity is

$$\mathbf{V}_{rod}\ (\phi > \phi_0) = \dot{s} + \Omega r\dot{\phi},$$

where $\dot{s}$ is given by equation (29).

The radial and tangential components, v_r and v_t, are given by

$$v_r = \dot{s}\cos\beta \quad \ldots\ldots\ldots\ldots\ldots\ldots \quad (31)$$

$$v_t = -\dot{s}\sin\beta + r\Omega = r(\dot{\beta} + \Omega). \quad \ldots\ldots\ldots \quad (32)$$

In equation (32) the term $-\dot{s}\sin\beta$ is positive because $\dot{s}$ is negative. It is interesting that the tangential velocity would be finite and positive for $\phi > \phi_0$, even if the mill were stationary. This is simply due to the increase in β as the rod slides down the surface of the lifter bar.

The magnitudes of the rod velocity and its radial and tangential components are illustrated in Fig. 7, which shows that these magnitudes (without regard to sign) are both monotonically increasing functions of time for as long as the rod is in contact with the lifter bar. The tangential component passes through a maximum at about 29 ms after the rod has passed through the equilibrium position, ϕ_0, and thereafter it decreases monotonically because r decreases as the rod slides down the surface of the lifter bar.

Since the lifter bar is of height h, the rod has to slide along its surface a distance $[(R-a)\cos\beta_0 - (R-h)]$ before reaching the edge. It does this in time t_L, which can be calculated from equation (29) with $s = R-h$, or this time can simply be read off from graphs of $\sigma(t)$ like that shown in Fig. 5, which refers to $\mu = 0$. For example, if $h = 20$ mm, then $t_L \approx 124$ ms.

Since ϕ_L, the angular position of the rod when it is as L, is given by

$$\phi_L = \Omega t_L + \theta_0 + \tan^{-1}\left(\frac{a + \frac{1}{2}d}{R-h}\right), \quad \ldots\ldots\ldots \quad (33)$$

the coordinates of the rod at t_L are

$$\begin{pmatrix} X_L \\ Y_L \end{pmatrix} = (R-h)\begin{pmatrix} \cos\phi_L \\ \sin\phi_L \end{pmatrix}, \quad \ldots\ldots\ldots\ldots \quad (34)$$

and its velocity components

$$\begin{pmatrix} V_{LX} \\ V_{LY} \end{pmatrix} = V_L\begin{pmatrix} \cos(\alpha_L + \phi_L) \\ \sin(\alpha_L + \phi_L) \end{pmatrix}, \quad \ldots\ldots\ldots\ldots \quad (35)$$

where $\phi_L = \tan^{-1} Y_L/X_L$

$$\alpha_L = \tan^{-1}\frac{r_L\Omega - \dot{s}\sin\beta}{\dot{r}_L} \quad \ldots\ldots\ldots\ldots \quad (36)$$

$$V_L^2 = \dot{r}_L^2 + (r_L\Omega - \dot{s}\sin\beta)^2. \quad \ldots\ldots\ldots\ldots \quad (37)$$

In equations (36) and (37), $\dot{r}_L = \dot{s}\cos\beta$, is the radial component of the velocity.

Thus, after travelling the full length of the lifter bar, the rod has an angular position of ϕ_L, and its coordinates and velocity are as given by equations (30) to (36). It then has to travel a further distance equal to the radius of one rod before it will be free of the lifter bar, and its angular position will be ϕ_F. (The subscript F denotes the limiting position at which the rod is just free of the lifter bar.)

TABLE II

CALCULATED ROD VELOCITIES AND ANGLES OF DEPARTURE IF SLIDING INTERACTIONS WITH LIFTER BARS ARE VALID

Height of lifter bar, h	Observed angle of departure	Calculated				
		Contact time, $t(h)$	Rod velocity at L, V_L	Rod velocity at F, V_F	Ratio of radial to transverse velocity components at F	Angle of departure ϕ_F
mm	degree	ms	mm·s^{-1}	mm·s^{-1}		degree
6,3	52 ± 3	52,4	753, 35,7°	718, 32,7°	0,12	51,3
12,7	67 ± 3	98,3	759, 7°	753, 3,2°	0,29	67,2
20,0	77 ± 3	123,9	775, −10,6°	789, −15,1°	0,55	76,2

Here it is assumed, to avoid discussion of a complicated rolling–slipping interaction at the edge of the lifter bar, that this additional distance was traversed with the rod in flight. This assumption introduces errors in the rod coordinates and velocity at point F, but it is believed they will be small because the duration of the interaction at the edge will be short. Under this assumption, the coordinates at F are

$$X_F \simeq X_L + V_{LX}a/V_L \text{ and} \quad \ldots\ldots\ldots\ldots (38)$$

$$Y_F \simeq Y_L + V_{LY}a/V_L - \tfrac{1}{2}ga^2/V_L^2, \quad \ldots\ldots\ldots\ldots (39)$$

where a/V_L is the time required for the rod to travel the distance a, which is equal to the radius of the rod.

The angle ϕ_F is given by

$$\phi_F = \tan^{-1} Y_F/X_F, \quad \ldots\ldots\ldots\ldots\ldots\ldots (40)$$

and the velocity components at F are

$$V_{FX} = V_{LX} \text{ and} \quad \ldots\ldots\ldots\ldots\ldots\ldots (41)$$

$$V_{FY} = V_{LY} - ga/V_L. \quad \ldots\ldots\ldots\ldots\ldots\ldots (42)$$

The radial component of the velocity at F is given by

$$\dot{r}_F = V_{FX} \cos \phi_F + V_{FY} \sin \phi_F. \quad \ldots\ldots\ldots\ldots (43)$$

With the aid of equations (30) to (43), the following can be predicted: the path of the rod while it is interacting with the lifter bar, its velocity in magnitude and direction at every point in the said path, and its angular position, coordinates, and velocity at the point F, when it is just free of the lifter bar.

The angles ϕ_F were calculated according to this procedure for various values of the coefficient of friction. Those obtained with zero friction are given in Table II.

Table II shows that, with $\mu = 0$, the calculated angles of departure, ϕ_F, are in excellent agreement with those measured. Calculations with μ finite showed that, if the sliding friction is increased to 0,1, the effect is to increase the angle of departure by about 5°. The best agreement was therefore obtained with $\mu = 0$. It is not unreasonable that the friction should be small. Table II also shows that, with the highest lifter bars, the radial component of the velocity is nearly 60 per cent of the transverse speed. This implies that, at the angle of departure, the calculated rod velocity is 789 mm · s^{-1} at an angle of about 15° south of west. This velocity is expected to be consistent, within the limits of experimental error, with that derived from the observed trajectory at that point. From the equations governing the flight of the rod, equations (15) and (16), it can be shown that the rod should have passed through ϕ_F at $t' \approx 6{,}25\ \tau$ with a velocity of V_T of about 840 mm · s^{-1} at an angle of 14° south of west. The discrepancy between the 'measured' and the calculated magnitudes of the velocity is about 6 per cent, and their directions are different by only 1°. These discrepancies are well accounted for by the experimental errors.

Further confirmation of the theory is obtained by the good agreement of the calculated trajectory (shown by T_F in Fig. 2), which was initiated with the calculated velocity, V_F (shown by the dotted curve between C and D in Fig. 2), with the observed trajectory (shown by the continuous curve). This is an important point of view of the fact that the calculated trajectory was determined purely by the 'initial conditions' at the point F.

The path of the rod while it is interacting with the lifter bar during its motion from B to C can be calculated from equations (31) and (28). The calculated path is shown by the dotted curve between these points in Fig. 2. It can be seen that this curve is in good agreement with the measured path, which is indicated by the rod positions 0 to 6 in the

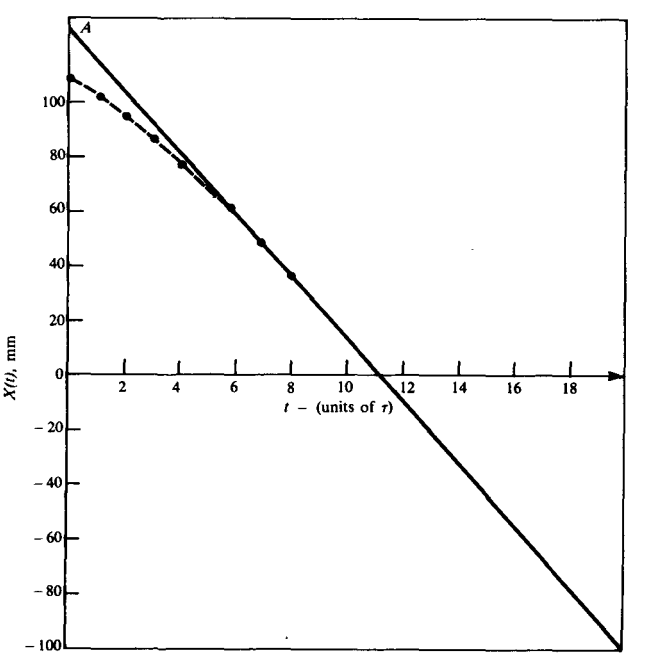

Fig. 8—Calculated time dependence of the *X* coordinate of a rod.

range B to C in that diagram. The small discrepancy between the calculated and measured rod positions in the range B to C is probably due to the surfaces of the lifter bar not being quite as symmetrical about the radius vector, s, as shown in Figs. 1 and 4.

Furthermore, the dependence on time of the X co-ordinate of the rod position can be computed from equation (31) and the calculated value of V_F. The calculated dependence is shown in Fig. 8. It can be seen that, for times less than t_F, the departure of the graph from the linear behaviour predicted by flight under the gravitational acceleration is remarkably similar to that observed experimentally and shown in Fig. 3.

It can be concluded that the sliding interaction gives a good quantitative description of the motion of a rod while it is interacting with a lifter bar, and that it correctly predicts its initial flight velocity in magnitude and direction. The subsequent motion of the rod is then under gravitational acceleration and along a well-defined parabolic trajectory.

A study was also made of the pure-rolling interaction between rods and lifter bars. A brief discussion, given in the Addendum, shows that this interaction does not account for the observed lift of lifter bars because it produces too much lift.

Accordingly, it it concluded that the measured lift of new lifter bars in the experimental mill is well accounted for by the interaction of rods with lifter bars in which the rods experience a normal reaction, and there is insufficient friction to promote pure-rolling motion, but the rods slide down the surface of the lifter bars after the latter have passed through the 'equilibrium angle', θ_0.

It must be pointed out that, if the friction were finite but small, the motion of the rod down the surface of the lifter bar, although dominated by slip, would consist of a combination of sliding and rolling. Under these conditions, the results obtained above would still be very nearly correct, because the velocities and angles at departure would not be much changed by a small coefficient of friction. Translation of the rod along the observed parabolic trajectory would be accompanied by spin about its long axis because the rod would have experienced an angular acceleration due to the friction torque exerted upon it while it was in contact with the lifter-bar surface. The rotational frequency associated with the spinning motion can be estimated from the relation

$$\tau_f = I_c \frac{d\omega}{dt}, \quad \ldots\ldots\ldots\ldots\ldots\ldots\ldots\ldots \quad (44)$$

where τ_f is the torque due to friction, I_c is the moment of inertia of the rod about its axis, and $\frac{d\omega}{dt}$ is its angular acceleration about the same axis. Since

$$\tau_f = a\mu\, mg \cos\theta(t),$$

$$I_c = \tfrac{1}{2}\, m\, a^2,$$

and

$$\frac{d\omega}{dt} = \frac{d\omega}{d\theta}\frac{d\theta}{dt} = \Omega \frac{d\omega}{d\theta},$$

it can be seen that the rotational frequency is

$$\nu = \frac{1}{2\pi} \int_0^{t_f} \frac{\tau_f}{I_c}\, dt$$

$$= \frac{\mu g}{\pi a \Omega} \int_{\theta_0}^{\theta_F} \cos\theta d\theta$$

$$= \frac{\mu g}{\pi a \Omega} [\sin\theta_F - \sin\theta_0]. \quad \ldots\ldots\ldots\ldots \quad (45)$$

If μ is 0,01, the spin of the rods when they come off the lowest lifter bars in the given mill will be about 18 r/min (and about 33 r/min for the highest lifter bars).

It is clear from the measurements of spin frequency, that it will be possible in future work for the coefficient of friction between the rods and lifter bars in any given mill to be determined. Such measurements were outside the scope of the present work, which was aimed at providing an understanding of the lifting mechanism. However, it is believed (as already suggested) that, in practice, the rod motion will consist of combined rolling and sliding. That the latter will dominate the motion is shown above by the excellent agreement between the observed and the calculated paths of a rod during its interaction with a lifter bar, and the observed and calculated trajectories.

In the present work, specific consideration was given to the influence of lifter bars of rectangular cross-section, i.e. new lifter bars. When a lifter bar becomes worn, its leading surface is at an angle, ψ say, to the old surface. The effect is to reduce the angle θ_0, at which equilibrium is achieved (by ψ), and hence the angle of departure, ϕ_F, of rods from the lining. McIvor has already shown that the wear of lifter bars has a profound effect on the trajectories of grinding elements in a rotary mill, but further discussion of these effects is beyond the scope of the present paper.

Summary and Conclusions

An analysis of the paths of the rods in an experimental mill that was fitted with lifter bars showed that, between the time when a rod departs from the shell, defined by the instant at which there is equilibrium between all the forces acting on the rod, and the instant that it departs from the lifter bar, there is an interaction between the rod and the lifter bar. This interaction has the following results for typical new lifter bars whose heights are about two-thirds of a rod diameter:

(a) the lift is about 20°, and
(b) the velocity of the rod at the point where flight is initiated is not only tangential to the circular motion, but it also has a finite and significant radial component.

The models of the interaction considered involved a pure rolling motion and sliding. The former predicted lift substantially larger than the lift that was measured, whereas the latter gave a good quantitative account of the dependence of the observed lift on the heights of lifter bars, and of the path of a rod while it is in contact with a lifter bar. The velocity of a rod at the point of projection calculated by the latter theory agreed, both in magnitude and direction, to within the limits of experimental error with that measured experimentally.

Quantitative descriptions were given of rod displace-

ment, velocity, and acceleration under the sliding interaction. It was anticipated that the general motion of a rod would consist in a combination of rolling and sliding, because the friction, although small, must be finite. Measurements of the resultant spin of a rod during its flight then led to a determination of the frictional forces that are operative while a rod is in contact with the surface of a lifter bar.

The flight paths of rods were analysed, and the trajectories were found to be parabolic and completely in accord with the predictions of elementary mechanics. This is in contra-distinction to the situation in ball and pebble mills, where difficulties were experienced in the reproduction of calculated trajectories[1,2].

Acknowledgements

Thanks are due to Dr P.T. Wedepohl (of Mintek) for encouragement and to Professor D.D. Howat, Mr M.J. Lazer, Mr D.I. Hoyer (also of Mintek), and Mr J.M. Keartland (student) for discussions. The author is indebted to Mr A. Hoernle (of the Nuclear Physics Research Unit of the University of the Witwatersrand) and Mr O. Pauw (of Mintek) for working through the algebra and physical details, and to Professor F.R.N. Nabarro F.R.S. (University of the Witwatersrand) for discussion and criticism. Mr Jan Hoek (Mintek) took the ciné photographs and Mr D.I. Stander made some apparatus available.

References

1. McIvor, R.E. Effects of speed and liner configuration on ball mill performance. *Min. Engng*, Jan. 1983. pp. 617-622.
2. Taggart, A.F. *Handbook of mineral dressing*. New York, Wiley, 1945. pp. 5.03-5.06.

Addendum: Rolling Interactions between Rods and Lifter Bars

The rolling interaction can be analysed with reference to Fig. 3. If torques about the point P are considered, it is found that

$$am\Omega^2 r \cos\beta - mga \sin(\Omega t + \theta_0) = I_p \frac{d\omega}{dt}, \quad \ldots \quad (1A)$$

where ω is the angular velocity of rotation of the rod in the clockwise sense (not indicated in Fig. 3) about its centre of mass and I_p is its moment of inertia about an axis through P. Since

$$\frac{d\omega}{dt} = \frac{1}{a}\frac{d^2s}{dt^2}, \quad \ldots \quad (2A)$$

$$I_p = \tfrac{3}{2} ma^2, \quad \ldots \quad (3A)$$

and

$$s(t) = r(t) \cos\beta(t), \quad \ldots \quad (4A)$$

the motion is given by

$$\frac{d^2s}{dt^2} - \tfrac{2}{3}\Omega^2 s = -\tfrac{2}{3} g \sin(\Omega t + \theta_0). \quad \ldots \quad (5A)$$

The boundary conditions are that, at $t = 0$, $s = s_0 = (R-a) \cos\beta_0$, and $\frac{ds}{st} = 0$ and $\theta = \theta_0$.

The solution consistent with the boundary conditions is

$$s(t) = \{(R-a)\cos\beta_0 - \frac{2g \sin\theta}{5\Omega^2}\} \cosh(\sqrt{\tfrac{2}{3}}\Omega t) - \frac{g}{5\Omega^2}\{\sqrt{6}\cos\theta_0 \sinh(\sqrt{\tfrac{2}{3}}\Omega t) - 2\sin(\Omega t + \theta_0)\}. \quad \ldots \quad (6A)$$

Given the angle θ_0, the subsequent analysis is similar to that already given in detail in connection with the sliding interaction. It has already been pointed out that the equilibrium angle, θ_0, is affected by the friction. The latter must be finite if pure rolling motion is to occur. This motion of the rod can be initiated when the lifter bar is at θ_0 if the coefficient of friction has at least the value of $\frac{1}{3}\tan\theta_0$. By the use of this value in equation (21), it is found that θ_0 is about 41,8° and the resulting angles of departure are as shown in Table III. (The subscript R is added to signify the rolling interaction.)

TABLE III

THE OBSERVED ANGLES OF DEPARTURE AND THOSE PREDICTED BY THE DYNAMICS OF ROLLING INTERACTION BETWEEN RODS AND LIFTER BARS

Height of lifter bar, h mm	Observed angle of departure, $\phi_F(h)$ degree	Calculated angle of departure, $\phi_{FR}(h)$ degree
6,3	53 ± 3	60,9
12,7	67 ± 3	76,0
20,0	73 ± 3	87,2

Table III shows that the angles of departure, and therefore the lift, predicted by a model of pure-rolling motion down the surface of a lifter bar are substantially larger than those observed experimentally. The differences are more than the experimental errors, which amount to only 3°. Therefore, the interaction in which a rod experiences a normal reaction and sufficient friction exists so that pure rolling motion down the surface of the lifter bar can occur cannot describe the observed lift of lifter bars, because such a mechanism predicts too much lift.